Charge Injection From Carbon Nanofibers Into Hexane Under Ambient Conditions

A. Ağıral, H. B. Eral, D. van den Ende, and J. G. E. Gardeniers

***Abstract*—The observation of charge injection from carbon nanofibers (CNFs) into liquid hexane under ambient conditions is reported. A CNF-coated electrode and a counter electrode are brought into micrometer proximity in a quasi-parallel geometry using a strain-gauge-based proximity sensor. Controlled charge injection is obtained at interelectrode distances of 4, 6, 9, and 15 μm. The resulting emission current shows an onset of about 3 V/μm, and it follows the Fowler–Nordheim behavior. The work reported here opens new applications for free electron chemistry in liquids and novel liquid field emitter devices.**

***Index Terms*—Charge injection, field emisssion, Fowler-Nordheim, free electron chemistry.**

FIELD EMISSION (FE) into liquids offers the possibility of controlled injection of a high current, permitting the estimation of electron mobilities [1], work-function measurements, and the study of electrochemical reactions in nonelectrolytes. Promoting electron transfer at the metal/liquid interface with high electric fields attracted early interest [2]–[5] since electrons were shown to exist in purified apolar organic liquids irradiated by ionizing radiations [6]–[8]. Charge injection from field-emitting cathodes was studied in order to understand the electron transport mechanism in connection with electrical breakdown in the liquids [9], [10] and chemical reactivity of electrons in apolar liquids [1]. In early studies, sharpened tungsten tips [1], [2], razor blades [3], or simple cylindrical brass electrodes [5] were used in order to produce an intense nonuniform electric field to the metal–dielectric interface with a distance of a few millimeters between the electrodes. The intensified field reduces the potential barrier height at that interface, which was already reduced with respect to vacuum, due to the higher dielectric constant of the liquid medium. This leads to a significant probability of electrons passing the barrier, either by Schottky, thermally aided field, or Fowler–Nordheim (FN) emission. Unlike in a solid, the electrons emitted in this way will not be trapped by fixed states but will move down the field gradient away from the emitter. When electrons gain enough energy to ionize the liquid atoms or molecules, charge-multiplication processes occur, which leads to space-charge-limited behavior. Therefore, the FN region in FE into liquids is quite narrow [1], [2].

The FE characteristics of nanostructures are of interest as their high aspect ratio provides local electric field enhancement, leading to electron emission at lower applied voltages [11]–[14]. Among the variety of existing nanostructures, carbon nanofibers (CNFs) exhibit outstanding FE performance with numerous applications, e.g., in cold cathodes for displays and other vacuum microelectronic devices [15], [16]. The use of CNF for charge injection in organic solvents has not been explored in great detail; the only related work that we are aware of is research in which nanostructured carbon was used for solvated electron generation in hexamethylphosphoric triamide (HMPA) [17]. HMPA is an aprotic polar solvent that has been used for the visualization of solvated electrons at room temperature because the solution will show an intense blue coloration. In this paper, we demonstrate charge injection from CNFs in hexane by bringing the electrode distance to micrometer-scale proximity. It is experimentally confirmed that an electrode coated with CNFs can be used to inject a high current into a dielectric liquid at low voltages, which opens the way for practical liquid FE devices.

CNFs were grown on 10-nm-thick nickel thin films which were deposited on standard n-type silicon chips (1 cm by 1 cm) with 10-nm tantalum as a barrier and adhesion layer. The chips were placed in a chemical vapor deposition setup and exposed to 27 sccm of C_2H_4 and 80 sccm of N_2 at 700 °C and atmospheric pressure for 20 min. A dense layer of CNFs with a diameter of 30–80 nm and a height of 2–3 μm is formed, as can be seen from the SEM image in Fig. 1 (bottom). Platinum of 200 nm was deposited by plasma sputtering at the back of the chip to make a low ohmic contact during testing.

In order to measure the charge injection current from a CNF-coated electrode, a stainless steel sphere, which acts as a counter electrode, was brought to micrometer proximity, using the experimental setup shown in Fig. 1 (top). The experimental setup relies on the Derjaguin approximation [18], [19]. The Derjaguin approximation is widely used in order to approximate the interaction between curved surfaces from a knowledge of the interaction for planar ones. This approximation intrinsically dictates that, as long as the range of the interactions,

Manuscript received March 15, 2011; revised May 20, 2011; accepted June 23, 2011. Date of publication August 4, 2011; date of current version September 21, 2011. This work was supported in part by the Technology Foundation STW, by the Applied Science Division of NWO, and by the technology program of the Ministry of Economic Affairs, The Netherlands, under Project 06626. The review of this paper was arranged by Editor A. C. Seabaugh.

A. Ağıral is with the Mesoscale Chemical Systems, MESA$^+$ Institute for Nanotechnology, Faculty of Science and Technology, University of Twente, 7500 AE, Enschede, The Netherlands, and also with the Lawrence Berkeley National Laboratory, Physical Biosciences Division, Berkeley, CA 94720 USA.

H. B. Eral and D. van den Ende are with the Physics of Complex Fluids, IMPACT Institute, University of Twente, 7500 AE Enschede, The Netherlands (e-mail: h.b.eral@utwente.nl).

J. G. E. Gardeniers is with the Mesoscale Chemical Systems, MESA$^+$ Institute for Nanotechnology, Faculty of Science and Technology, University of Twente, 7500 AE Enschede, The Netherlands.

Color versions of one or more of the figures in this paper are available online at http://ieeexplore.ieee.org.

Digital Object Identifier 10.1109/TED.2011.2160947

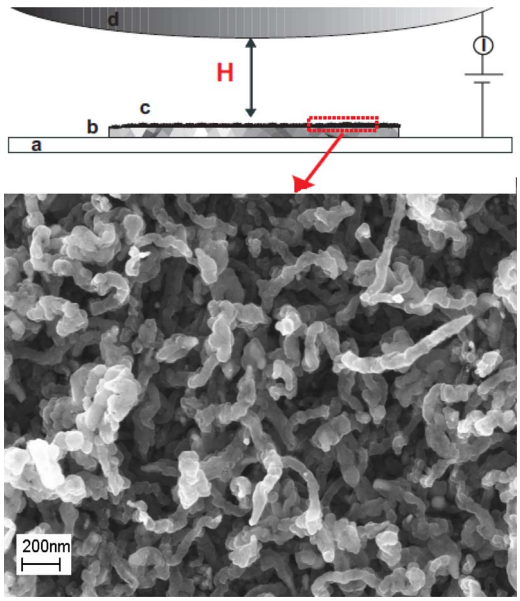

Fig. 1. (Top) Illustration of the experimental configuration where H is the interelectrode distance. Essential parts of the setup are the following: (a) ITO-coated glass container filled with liquid hexane, (b) chip electrode coated with CNFs, (c) surface of the cathode with CNFs, and (d) spherical stainless steel counter electrode. (Bottom) SEM image of CNFs grown on nickel thin film on silicon.

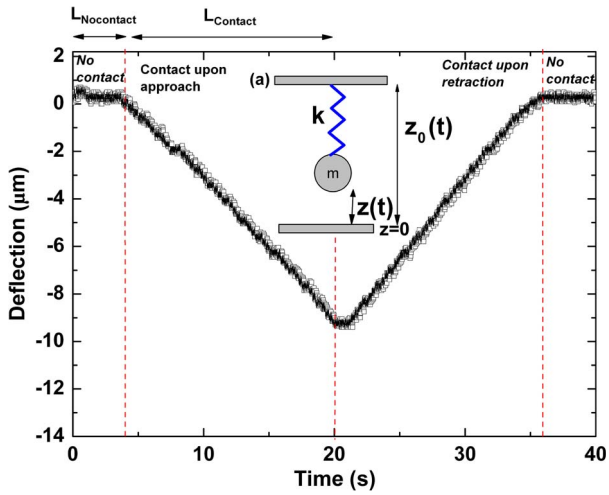

Fig. 2. Deflection versus time curve obtained from a strain-gauge-based proximity sensor. The solid red line indicates the theoretical prediction obtained from solving (3). Inset illustrates the mass-spring system used in modeling of the proximity sensor (see text).

the size of the object of interest, and the separation distance are much smaller than the curvature of the sphere, the sphere can be treated as a planar object. In the experimental setup described here, the area of interest and the characteristic size of the CNFs are a lot smaller than the diameter of the sphere ($d_{\text{sphere}} = 20$ mm), so that, at the relevant scale, the geometry can be treated as that of quasi-parallel planes. The setup consists of a sample chamber, a proximity sensor, and a current measurement system. The sample chamber is a custom-made glass chamber, where the bottom of the chamber is of ITO-coated glass. The CNF-coated electrode was attached on this ITO-coated glass surface with conductive glue, and the chamber was filled with liquid hexane (anhydrous, $\geq$ 99% Sigma-Aldrich). The proximity sensor consists of a piezo stage and microscrews to move the setup, a Wheatstone bridge of four strain gauges glued on cantilevers to measure bending, a lock-in amplifier to eliminate noise, and a data acquisition (DAQ) card to simultaneously control the piezo stage and record the voltage output of the bridge (ΔV_{bridge}). Bending of the cantilevers leads to a change in the resistance of the strain gauges, and with that, a proportional change in ΔV_{bridge} will be generated and recorded by the DAQ card [20], [28]. To reach a certain interelectrode distance H (see Fig. 1), a touch-and-retract procedure was applied. As shown in Fig. 2, at contact, pushing the spherical electrode toward the plane gives a continuous increase (denoted as "contact upon approach") or decrease in deflection ("contact upon retraction"). Using the microscrews and the strain gauge signal in combination, the sphere electrode can be positioned at a defined distance (H) within 0.2-μm accuracy. The H value is calculated from a deflection-versus-time graph in Fig. 2, as it is the ratio of the deflection signal during contact (denoted by L_{contact} in Fig. 2) to the flat signal region (denoted by $L_{\text{nocontact}}$), multiplied by the piezo range averaged over approach and retraction

$$H = \frac{L_{\text{contact}}}{L_{\text{contact}} + L_{\text{Nocontact}}} * PI_{\text{range}}. \tag{1}$$

Once the interelectrode distance is fixed, a negative voltage is applied to the CNF-coated electrode. Voltage–current data were measured with a Keithley 237 source meter unit. Electrodes and chamber are rigorously rinsed with fresh hexane before each experiment. We also conducted control experiment with electrodes without CNFs. These control experiments produced no measurable current even under the highest voltages applied.

A theoretical analysis of the sphere motion was performed in order to understand the response of the proximity sensor. The distance sensor can be considered as a simple mass-spring system with mass (m) and spring constant (k) (see inset (a) in Fig. 2). The equation of motion can be derived from a force balance

$$m\frac{\partial^2 z}{\partial t^2} = k\left(z_0(t) - z\right) + F_{\text{liq}}. \tag{2}$$

The force acting on the liquid (F_{liq}) is balanced by the force imposed by the cantilevers modeled as a spring, $k(z_0(t) - z)$. The vertical position of the sphere at a given time t is denoted by z and the reference position of the piezo stage by $z_0(t)$. The force acting on the liquid is given by

$$\mathrm{F}_{\text{liq}} = -6\pi\mu a\left(1 + \frac{a}{z}\right)\frac{\partial z}{\partial t} \tag{3}$$

where μ and a are the liquid viscosity and the sphere radius, respectively. Equation (3) is an approximation of the Reynolds force [19], which is accurate in the vicinity of the wall ($a/z \ll 1$) and very far away from the wall ($a/z \gg 1$). Combining (2) and (3) and inserting a nondimensional position as $\zeta = z/a$ and

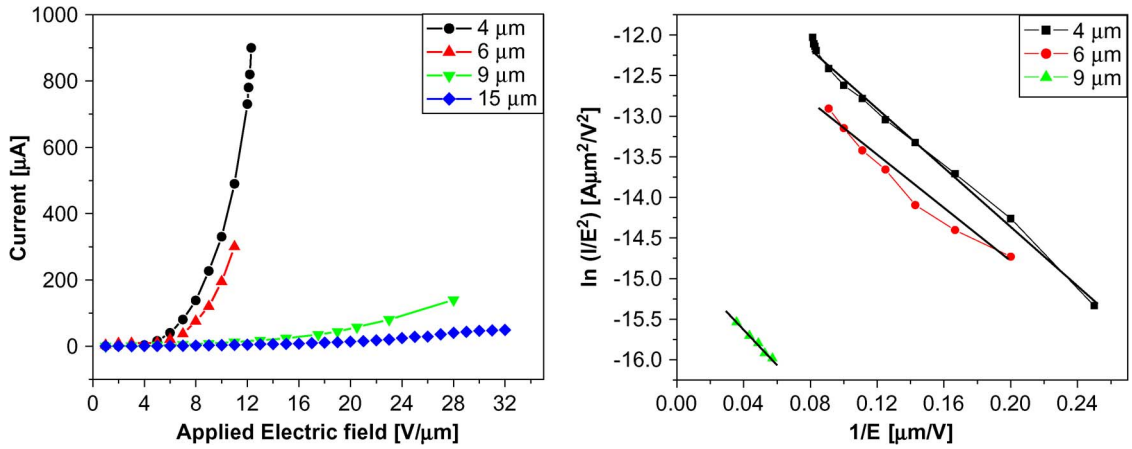

Fig. 3. Charge injection properties of CNFs measured in liquid hexane. (a) Current (I) versus electric field (E) curves obtained by applying negative voltages to the CNF emitter at the indicated electrode distances. (b) Corresponding FN plots.

a nondimensional time as $\tau = t/t_0$, the following expression is obtained:

$$\zeta_0(\tau) = \ddot{\zeta} + \beta\left(1 + \frac{1}{\zeta}\right)\dot{\zeta} + \zeta \tag{4}$$

where ζ is now a function of τ, $t_0 = \sqrt{m/k}$, and $\beta = 6\pi\mu a(t_0/m)$. It is crucial to understand the force response as it depends not only on the approach velocity $(\partial z/\partial t)$ but also on the viscosity of the system. Both parameters have to be chosen with care so that the viscous forces can be ignored to simplify the determination of the position (H) from the force response with (1). The theoretical and experimental curves in Fig. 2 agree well, indicating that the motion of the sphere follows our modeling and that the response signal can be converted to distance reliably.

Fig. 3 shows the curves of the measured current (I) as a function of the applied electric field (E) for different inter-electrode distance values (H). These curves were obtained by applying a negative voltage to the CNF-coated emitter. It can be seen that, in particular for the curve obtained for a distance of 4 μm, the current slowly increases with increasing electric field at low fields, with a steep rise when the electric field exceeds 3 V/μm. The exponential increase is characteristic for the FE into hexane, as can be seen from the other curves (except for the 15-μm electrode distance). These electron emission characteristics were evaluated by standard FN tunneling theory, using the following current–density equation [21]:

$$J = \left[\tau_F^{-2}\alpha\varphi^{-1}F^2\right]\exp(-v_F\varepsilon\varphi^{3/2}F^{-1}) \tag{5}$$

where $\alpha = e^3/8\pi h_p = 1.541434 \times 10^{-6}$ A $\cdot$ eV $\cdot$ V^{-2}, $\varepsilon = (8\pi/3)(2m_e)^{1/2}/eh_p = 6.830890 \times 10^9$ eV$^{-3/2}$ $\cdot$ V $\cdot$ m^{-1}, e is the elementary positive charge, m_e is the electron mass, h_p is Planck's constant, J is the local current density, F is local electric field, φ is the local work function of the emitting surface, and τ_F and v_F are the values of τ (decay rate correction factor) and v (tunneling exponent correction factor), respectively, which apply to a barrier of unreduced height h equal to the local work function φ. The correction factors are considered to be equal to unity for the elementary triangular barrier.

Geometric field enhancement at the tips of the CNFs will increase the local field F to make it higher than F_M by a factor γ which is called the field enhancement factor

$$\gamma = F/F_M. \tag{6}$$

Using the macroscopic electric field F_M as an FN variable in (5) to replace F and writing the emission current I as $I = A_N J$ (where A_N is the notional emission area; here, we assume a uniform local work function), the following equation arises [22], [23]:

$$\ln\left[I/F_M^2\right] = \ln\left[A_N\tau_F^{-2}\alpha\varphi^{-1}\gamma^2\right] - \left[v_F\varepsilon\varphi^{3/2}/\gamma\right]/F_M. \tag{7}$$

Assuming that the hexane behaves as a classical dielectric, the image potential on CNFs is reduced by $1/\varepsilon_r$, (permittivity, $\varepsilon_r = 1.89$). Equation (7) shows that, at a specific value of the macroscopic field and assuming a triangular barrier, the slope of a plot according to (7) is equal to $b\varphi^{3/2}/\gamma$ [22]. The equation is valid for FE into dielectric liquids [24], [25] if φ is replaced by φ_1

$$\varphi_1 = \varphi + \Delta\varphi. \tag{8}$$

The vacuum work function of graphite is 5 eV, but the presence of hexane at the surface of the CNFs influences the work done for FE. Generally, the change $(\Delta\varphi)$ in the value of the vacuum work function (φ) depends on the electrical double layer at the surface and the electron immersion energy [26]. The final energy state of the electrons will be the immersion energy in the hexane, and the work function will be reduced by this electron immersion energy. This energy reduction was found to be 0.02–0.09 eV [27]. Therefore, the modified work function (φ_1) for CNFs in hexane is equal to 4.91–4.98 eV. Fig. 3(b) shows the FN plots, corresponding to (7), for the different electrode distances. If we assume that the emission comes from one band with $\varphi_1 = 4.91$ eV, the field enhancement factors are estimated from the FN plots to be ca. 4105, 3308, and 3730 for 4-, 6-, and 9-μm electrode distances, respectively. For the 15-μm electrode distance, we did not reach a high enough electric field values to establish whether true FN FE occurs at this distance. For sufficiently high electric field values, the space charge effects in liquid hydrocarbons start to play an important role, and the charge injection mechanism changes its character from the FE

(FN) to a space-charge-limited current. In our measurements, we have not reached high enough electric fields required for the observation of this space-charge-limited regime.

Application of the experimental method utilized (strain gauges) in bringing two electrodes together described in this work is essential due the difficulties associated with utilizing optical techniques such as interferometry with rough opaque surfaces. However, caution has to be taken while applying the method as it involves contact of two surfaces. The spring constant of the cantilevers to which the strain gauges are attached is 72 N/m. For 1-μm deflection, the cantilevers apply 72-μN force on the contact, which is too low to cause significant elongation or deformation on CNTs (Young modulus of single walled CNTs: 1000 GPa) but may cause deformation for soft materials. Another concern is the applicability of the Derjaguin approximation and the homogeneity of the electric field; to check this, we need to define a length scale of interest. Our measurements indicate that the vertical length scale of interest is not larger than 15 μms as we see no field enhancement at $H = 15$ μm. The variation of height, 15 μm away from the apex of the sphere, is 0.06 μm well below the smallest H considered. Even extending this length scale to 100 μm, H varies less than 0.25 μm, which is an order of magnitude smaller than the smallest H considered. Furthermore, as opposed to vacuum experiments, the liquid hexane is prone to contamination. For this reason, fresh hexane is used for each set of experiments, and the setup is isolated by a Plexiglas container. The data shown in Fig. 3 could not be repeated on the same sample with different heights, as the sample shows arc formation and breakdown. Hence, the substrate was not usable after one measurement. When we changed the damaged substrate with a fresh one, we obtained quantitatively same results. Breakdown of the substrate is the major factor that limited the statistical accuracy of our measurements [29].

In summary, we present a strain-gauge-based method to bring two electrodes to micrometer-scale proximity and use this method to demonstrate charge injection from CNFs into liquid hexane under ambient conditions. Emission currents obey the FN equation, with a turn-on field of 3 V/μm for the case with an electrode distance of 4 μm. Emission current decreased when the electrode distance increased from 4 to 9 μm. The presented method of charge injection into dielectric liquids with the aid of carbon nanostructures under ambient conditions may initiate interesting applications in electrochemical synthesis or free electron chemistry with solvated electrons, as well as in the development of practical field-emission electronic devices.

ACKNOWLEDGMENT

The authors would like to thank K. Smit for technical assistance. H. B. Eral and A. Agiral contributed equally to the presented work.

REFERENCES

[1] B. Halpern and R. Gomer, "Field emission in liquids," *J. Chem. Phys.*, vol. 51, p. 1031, 1969.

[2] K. Dotoku, H. Yamada, S. Sakamoto, S. Noda, and H. Yoshida, "Field emission into nonpolar organic liquids," *J. Chem Phys.*, vol. 69, no. 3, pp. 1121–1125, Aug. 1978.

[3] G. Coe, J. F. Hughes, and P. E. Secker, "High-current injection into liquid hexane using field emitters," *Brit. J. Appl. Phys.*, vol. 17, no. 7, pp. 885–890, Jul. 1966.

[4] W. R. Lepage and L. A. Dubridge, "Electron emission into dielectric liquids," *Phys. Rev.*, vol. 58, no. 1, pp. 61–66, Jul. 1940.

[5] W. B. Green, "Controlled field emission in hexane," *J. Appl. Phys.*, vol. 27, no. 8, pp. 921–925, Aug. 1956.

[6] P. H. Tewari and G. R. Freeman, "Dependence of radiation-induced conductance of liquid hydrocarbons on molecular structure," *J. Chem. Phys.*, vol. 49, no. 10, pp. 4394–4399, Nov. 1968.

[7] R. M. Minday, L. D. Schmidt, and H. T. Davis, "Free electrons in liquid hexane," *J. Chem. Phys.*, vol. 50, no. 3, pp. 1473–1474, Feb. 1969.

[8] W. F. Schmidt and A. O. Allen, "Mobility of free electrons in dielectric liquids," *J. Chem. Phys.*, vol. 50, no. 11, p. 5037, Jun. 1969.

[9] R. Tobazeon, "Prebreakdown phenomena in dielectric liquids," *IEEE Trans. Dielectr. Elect. Insul.*, vol. 1, no. 6, pp. 1132–1147, Dec. 1994.

[10] A. Denat, J. P. Gosse, and B. Gosse, "Electrical conduction of purified cyclohexane in a divergent electric field," *IEEE Trans. Elect. Insul.*, vol. 23, no. 4, pp. 545–554, Aug. 1988.

[11] W. A. De Heer, A. Chatelaine, and D. Ugarte, "A carbon nanotube field-emission electron source," *Science*, vol. 270, no. 5239, pp. 1179–1180, Nov. 1995.

[12] P. G. Collins and A. Zettl, "A simple and robust electron beam source from carbon nanotubes," *Appl. Phys. Lett.*, vol. 69, no. 13, pp. 1969–1971, Sep. 1996.

[13] A. Agiral, A. W. Groenland, J. K. Chinthaginjala, K. Seshan, L. Lefferts, and J. G. E. Gardeniers, "On-chip microplasma reactors using carbon nanofibres and tungsten oxide nanowires as electrodes," *J. Phys. D, Appl. Phys.*, vol. 41, no. 19, p. 194 009, Oct. 2008.

[14] A. Agiral and J. G. E. Gardeniers, "Synthesis and atmospheric pressure field emission operation of W18O49 nanorods," *J. Phys. Chem. C*, vol. 112, no. 39, pp. 15 183–15 189, Sep. 2008.

[15] W.-B. Choi, D.-S. Chung, J. H. Kang, H. Y. Kim, Y. W. Jin, I. T. Han, Y. H. Lee, J. E. Jung, N. S. Lee, G. S. Park, and J. M. Kim, "Fully sealed, high-brightness carbon-nanotube field-emission display," *Appl. Phys. Lett.*, vol. 75, no. 20, pp. 3129–3131, Nov. 1999.

[16] Q. H. Wang, A. A. Setlur, J. M. Lauerhaas, J. Y. Dai, E. W. Seeling, and R. P. H. Chang, "A nanotube-based field-emission flat panel display," *Appl. Phys. Lett.*, vol. 72, no. 22, pp. 2912–2913, Jun. 1998.

[17] A. G. Krivenko, N. S. Komarova, and N. P. Piven, "Electrochemical generation of solvated electrons from nanostructured carbon," *Electrochem. Commun.*, vol. 9, p. 2364, 2007.

[18] B. V. Derjaguin, "Friction and adhesion," *Kolloid Z.*, vol. 69, p. 15, 1934.

[19] J. Israelachvili, *Intermolecular and Surface Forces*. London, U.K.: Academic, 1992.

[20] H. B. Eral, D. van den Ende, F. Mugele, and M. H. G. Duits, "Influence of confinement by smooth and rough walls on particle dynamics in dense hard-sphere suspensions," *Phys. Rev. E, Stat. Phys. Plasmas Fluids Relat. Interdiscip. Top.*, vol. 80, no. 6, p. 061 403, Dec. 2009.

[21] R. G. Forbes and J. H. B. Deane, "Reformulation of the standard theory of Fowler–Nordheim tunnelling and cold field electron emission," *Proc. R. Soc. A*, vol. 463, no. 2087, pp. 2907–2927, Nov. 2007.

[22] R. G. Forbes, "Field emission: New theory for the derivation of emission area from a Fowler–Nordheim plot," *J. Vac. Sci. Technol. B, Microelectron. Nanometer Struct.*, vol. 17, no. 2, pp. 526–533, Mar. 1999.

[23] R. G. Forbes, "Low-macroscopic-field electron emission from carbon films and other electrically nanostructured heterogeneous materials: Hypotheses about emission mechanism," *Solid State Electron.*, vol. 45, no. 6, pp. 779–808, Jun. 2001.

[24] B. Halpern and R. Gomer, "Field emission and field ionization," *J. Chem. Phys.*, vol. 43, p. 1069, 1965.

[25] R. Gomer, "Field emission and field ionization in condensed phases," *Acc. Chem. Res.*, vol. 2, p. 41, 1972.

[26] H. House, "High field conduction currents in hexane," *Proc. Phys. Soc. B*, vol. 70, no. 10, pp. 913–927, Oct. 1957.

[27] R. A. Holroyd and M. Allen, "Energy of excess electrons in nonpolar liquids by photoelectric work function measurements," *J. Chem. Phys.*, vol. 54, no. 12, pp. 5014–5021, Jun. 1971.

[28] H. B. Eral, J. M. Oh, M. Duits, D. van den Ende, and F. Mugele, "Anisotropic and hindered diffusion of colloidal particles in a closed cylinder," *Langmuir*, vol. 26, no. 22, pp. 16 722–16 729, Nov. 2010, DOI:10.1039/C1SM05183K.

[29] H. B. Eral, D. Mampallil, M. Duits, and F. Mugele, "Suppressing the coffee stain effect: How to control colloidal self-assembly in evaporating drops using electrowetting," *Soft Matter*, vol. 7, pp. 4954–4958, 2011.

A. Ağıral, photograph and biography not available at the time of publication.

H. B. Eral, photograph and biography not available at the time of publication.

D. van den Ende, photograph and biography not available at the time of publication.

J. G. E. Gardeniers, photograph and biography not available at the time of publication.